Electronic Supplementary Material (ESI) for Catalysis Science & Technology.

Supporting Information

Palladium Islands on Iron Oxide Nanoparticles for Hydrodesulfurization Catalysis

Ali Mansouri, Natalia Semagina*

Department of Chemical and Materials Engineering, University of Alberta, 9211-116 St., Edmonton, AB T6G 1H9, Canada. * semagina@ualberta.ca

Nomenclature:

Parameter	Description	Unit
ρ_b	catalyst bed density	kg/m^3
ρ_c	catalyst compact bulk density	kg/m^3
ρ_g	gas density	kg/m^3
ϕ	catalyst bed porosity	
μ	feed viscosity	kg/m.s
ε_p	catalyst particle porosity	
τ	catalyst tortuosity	
b	bed dilution	
Bi_w	Biot number at the reactor wall	
C_i	initial concentration of 4,6-DMDBT in feed stream	mol/L
$C_{Ab} \approx C_{As}$	bulk (and surface) 4,6-DMDBT gas phase concentration	mol/m^3
d_t	reactor internal diameter	m
d_p	catalyst particle diameter	m
d_{pore}	catalyst pore diameter	nm
D_{AB}	4,6-DMDBT diffusivity in H_2	m^2/s
D_k	Knudsen diffusivity	m^2/s
D_{pore}	diffusivity in a pore	m^2/s
D_e	effective diffusivity	m^2/s
E_a	activation energy	kJ/mol
F_i	inlet molar flow rate of 4,6-DMDBT	mol/s
H_{rxn}	heat of reaction	kJ/mol
h	heat transfer coefficient	kW/m^2.K
k_i	observed reaction rate constant	L/kg.s

k_c	mass transfer coefficient	m/s
k_{H2}	thermal conductivity of hydrogen	W/m.K
L_{bed}	catalyst bed length	m
$m_{cat.}$	mass of catalyst in the reactor	kg
M	molecular weight of 4,6-DMDBT	g/mol
n	reaction order	
Nu	Nusselt number	
p	number of catalyst layers	
P	operating pressure	atm or Pa
$-r_{A(obs)}$	observed reaction rate	mol/kg.s
$-r_{v(obs)}$	observed reaction rate per unit of particle volume	mol/m^3.s
R	catalyst particle radius	m
R_g	universal gas constant	J/mol.K
Re	Reynolds number	
R_t	Reactor internal radius	m
S	BET surface area	m^2/g
Sh	Sherwood number	
T	reaction temperature	K
T_w	Reactor wall temperature	K
U	fluid superficial velocity	m/s
v_i	molar diffusion volume	cm^3/mol
X_i	4,6-DMDBT HDS conversion	

Table S1. Calculations on the absence of internal and external mass and heat transfer limitations and near-ideal plug flow behavior; the required parameters and calculation procedure are listed in Table S2.

Phenomenon	**criterion**	**calculated value for the criterion**
external heat transfer limitations [S1]	$\Delta T_{film} = \frac{-r_{A(obs)} \times \rho_b \times R \times E_a \times (-\Delta H_{rxn})}{R_g \times h \times T^2} < 0.15$	$2.6 \times 10^{-6} < 0.15$
external mass transfer limitations (Mears criterion) [S1]	$\frac{-r_{A(obs)} \times R \times n \times \rho_b}{k_c \times C_{Ab}} < 0.15$	$7.8 \times 10^{-4} < 0.15$
internal mass transfer limitations (Weisz-Prater criterion for the 1st order reaction) [S1]	$\frac{-r_{A(obs)} \times R^2 \times \rho_c}{D_e \times C_{As}} < 0.3$	$0.03 < 0.3$
plug-flow behavior (no axial dispersion and wall effects) [S2, S3]	$\frac{d_t}{d_p} > 10$ $\frac{L_{bed}}{d_p} > 50$	$127 > 10$ $162 > 50$
Radial temperature gradient	$\frac{-r_{v(obs)} \times (1-\varepsilon) \times (1-b) \times E_a \times (-\Delta H_{rxn}) \times R_t^2}{R_g \times T_w^2 \times k_{H2}} \times$	$6.2 \times 10^{-4} < 0.05$
effect of bed dilution [S6]	0.6b/2p < experimental error 0.1	0.042

Table S2. Calculation of parameters in Table S1 for $FeO_x@Pd_{0.2}/Al_2O_3$ catalyst.

Parameter	Definition and Unit	Equation and Value
$k_{i(obs)}$	Observed rate constant @ 623 K and 4,6-DMDBT conversion of 35.9 % ($X_{4,6\text{-DMDBT}}$) [L/kg.s]	$k_i = \frac{Ln\left(\frac{1}{1-X_i}\right) \times F_i}{C_i \times m_{cat.}} = 2.06 \times 10^{-3}$
$-r_{A(obs)}$	Observed reaction rate @ 623 K and $X_{4,6\text{-DMDBT}}$ = 35.9 % [mol/kg.s]	$-r_{A(obs)} = k_i \times C_i = 3.5 \times 10^{-5}$
$m_{cat.}$	mass of catalyst in the reactor [g]	0.18
F_i	4,6-DMDBT molar flow rate [mol/s]	1.41×10^{-8}
C_i	Initial concentration of 4,6-DMDBT [mol/L]	0.017
ρ_c	Catalyst compact bulk density [kg/m^3]	4000
ϕ	Catalyst bed porosity	0.4
ρ_b	Catalyst bed density [kg/m^3]	$\rho_b = (1 - \phi) \times \rho_c = 2400$
R	Catalyst particle radius [m]	0.00005
E_a	Activation energy for the 1st order gas phase reaction [kJ/mol]	200 [S1]
ΔH_{rxn}	Heat of reaction calculated from the enthalpies of formation of each compounds in Scheme 1 provided in ref. [S4], [kJ/mol]	-148.5
Rg	Universal gas constant [J/mol.K]	8.314
T	Reaction temperature [K]	623
d_p	Catalyst particle diameter [m]	0.0001
ρ_g	hydrogen gas density at 623 K and 3 MPa, [kg/m^3]	1.17
μ	hydrogen viscosity at 623 K [kg/m.s]	1.42×10^{-5}
Re	Reynolds number at 623 K for the fluid velocity of 0.022 m/s (in the reactor i.d. 0.5") assuming the bed porosity of 0.4	$Re = \frac{U \times \rho_g \times d_p}{(1 - \phi) \times \mu} = 0.18$
Sh, Nu	Sherwood and Nusselt numbers	2.0

k_{H2}	Thermal conductivity of hydrogen at 623 K, [W/m.K]	0.25
h	Heat transfer coefficient [kW/m^2.K]	$h = \frac{Nu \times k_{H2}}{d_p} = 1.5$
n	Reaction order, HDS of 4,6-DMDBT on Pd-based catalyst is known to follow a pseudo-first-order kinetics [S5]	1.0
$C_{Ab} \approx C_{As}$	Bulk 4,6-DMDBT gas phase concentration considering hydrogen gas [mol/m^3]	0.107
M	4,6-DMDBT molecular weight [g/mol]	212.3
D_{AB}	Estimated gas phase 4,6-DMDBT diffusivity in H_2 at 623 K and 3 MPa [m^2/s]; the molar volumes of H_2 and 4,6-DMDBT are 7.07 and 271.76 cm^3/mol, respectively.	$D_{AB} = \frac{10^{-3}\ T^{1.75}\left[\frac{1}{M_A} + \frac{1}{M_B}\right]^{0.5}}{P\left[\left(\sum v_i\right)_A^{1/3} + \left(\sum v_i\right)_B^{1/3}\right]^2} = 2.61 \times 10^{-6}$
k_c	Mass transfer coefficient [m/s]	$k_c = \frac{D_{AB} \times Sh}{d_p} = 0.05$
d_{pore}	Catalyst pore diameter [nm]	5.8
D_k	Knudsen diffusivity [m^2/s]	$D_K = 48.5\ \times\ d_{pore} \times \sqrt{\frac{T}{M}} = 4.8 \times 10^{-7}$
D_{pore}	Diffusivity in a pore [m^2/s]	$D_{pore} = \left(\frac{1}{D_{AB}} + \frac{1}{D_K}\right)^{-1} = 4.1 \times 10^{-7}$
S	BET surface area [m^2/g]	155
ε_p	Catalyst particle porosity	$\varepsilon_p = \frac{S\ \times \rho_c \times d_{Pore}}{4} = 0.9$
τ	Catalyst tortuosity	3.9
D_e	Effective diffusivity [m^2/s]	$D_e = \frac{\varepsilon_P \times D_{pore}}{\tau} = 9.5 \times 10^{-8}$
d_t	Reactor internal diameter [m]	0.0127
L_{bed}	Catalyst bed length [m]	0.0162
b	Bed dilution [-]: 3.96 g SiC (density 3.21 g/cm^3), 0.18 g Al_2O_3 (density 3.95 g/cm^3)	0.964

l	Length of undiluted bed [m], 0.18 g Al_2O_3 (density 3.95 g/cm^3), 0.4 bed porosity, 0.0127 m diameter	0.0006
p	Number of catalyst layers [S6]	$p=1.1547\ (l/d_p) = 6.93$
Bi_w	Biot number at the reactor wall	$Bi_w = \frac{h \times d_p}{k_{H2}} = 0.6$
$-r_{v(obs)}$	Observed reaction rate @ 623 K and $X_{4,6\text{-}DMDBT}$ = 35.9 % [mol/m^3.s]	$-r_{v(obs)} = -r_{A(obs)} \times \rho_c = 0.14$

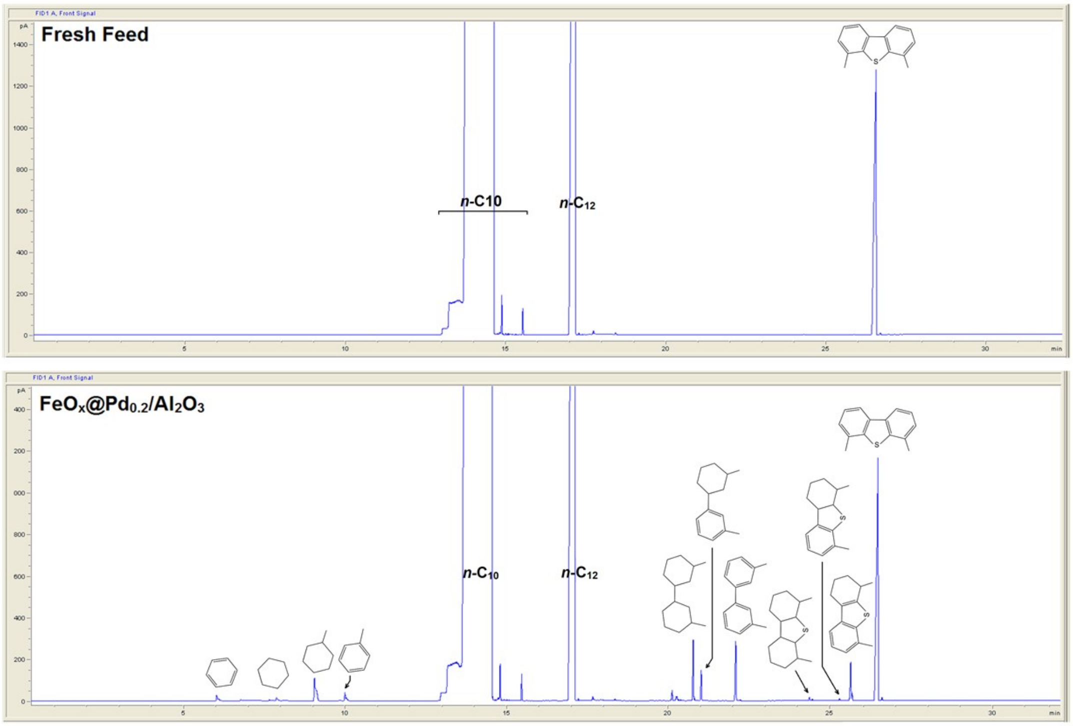

Figure S1. Typical GC chromatograms of fresh feed and HDS products at 623 K and 3 MPa over $FeO_x@Pd_{0.2}/Al_2O_3$ catalyst collected after 18 h on stream. The hydrocracking product identification was performed by GC-MS:

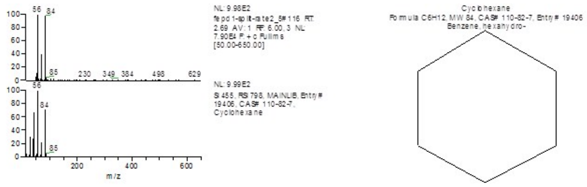

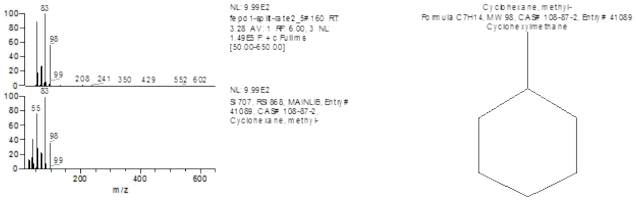

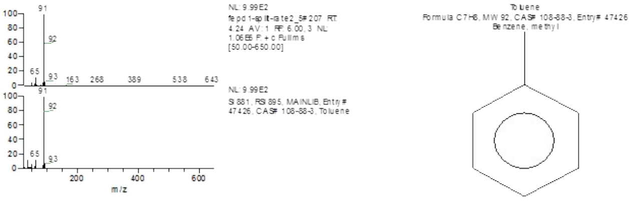

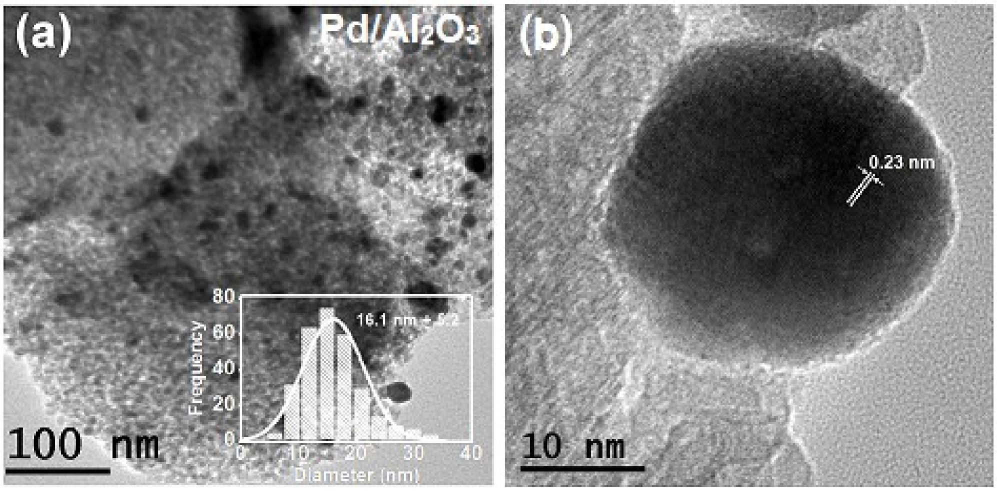

Figure S2. TEM (a) and HRTEM (b) images of spent Pd/Al_2O_3 catalyst.

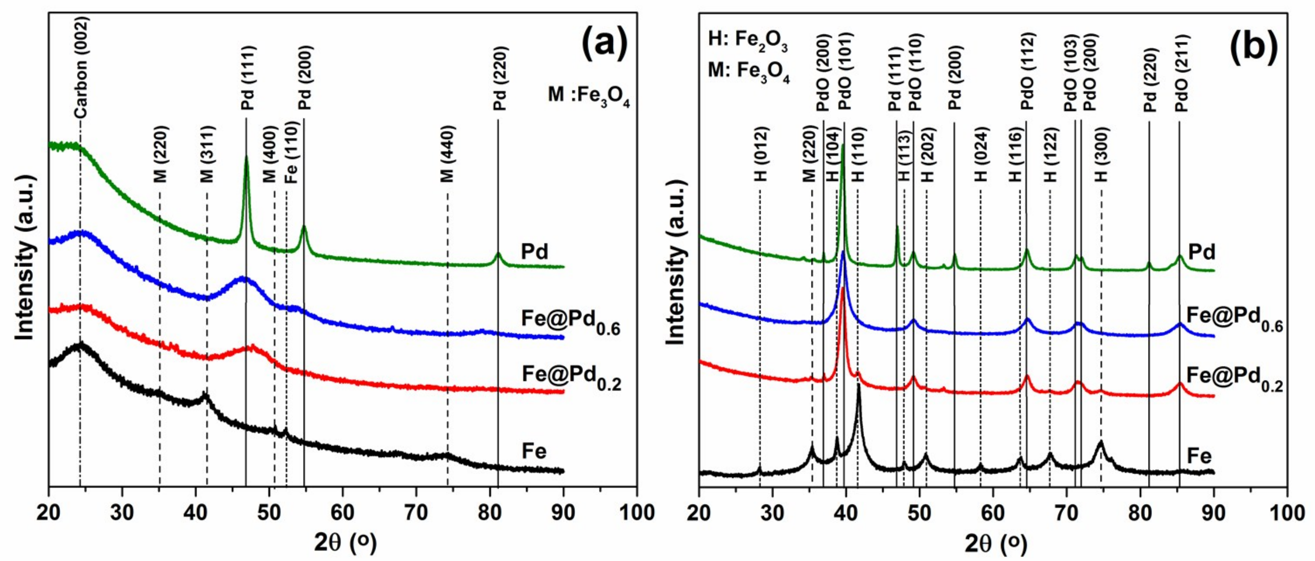

Figure S3. (a) XRD patterns of unsupported FeO_x, Pd, and $FeO_x@Pd$ nanoparticles after synthesis, and (b) after 4 h of calcination at 673 K; M and H represent magnetite (Fe_3O_4) and hematite (Fe_2O_3), respectively. The peaks were assigned based on the powder diffraction file numbers 00-019-0629 for magnetite, 97-002-2505 for hematite, 00-006-0696 for metallic iron, 97-018-0870 for metallic palladium, and 00-006-0515 for PdO. Figure S3(a) was used to calculate the lattice parameters in Table 1. The high intensities at 20-30° range in Figure S3(a) are due to carbon in PVP (stabilizer), which disappeared after calcination in Figure S3(b).

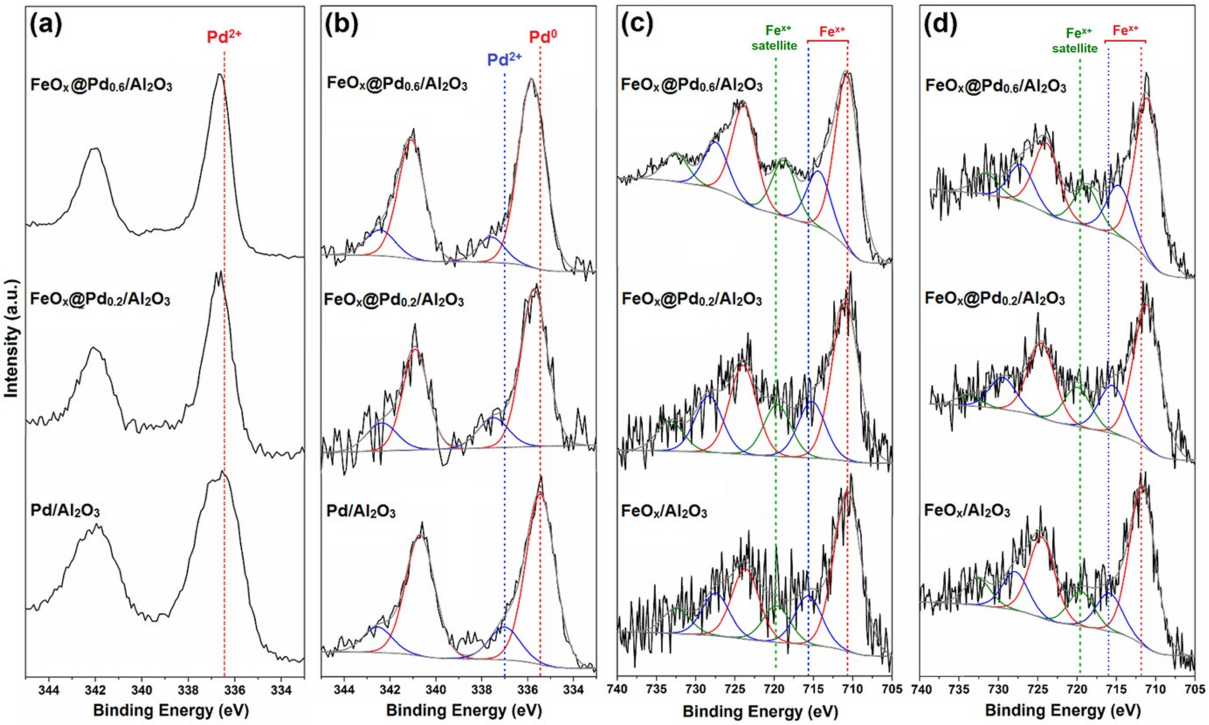

Figure S4. XPS profiles of Pd/Al$_2$O$_3$, FeO$_x$/Al$_2$O$_3$ and FeO$_x$@Pd$_n$/Al$_2$O$_3$ catalysts: Pd 3d of calcined (a) and spent (b) catalysts; Fe 2p of calcined (c) and spent catalysts (d).

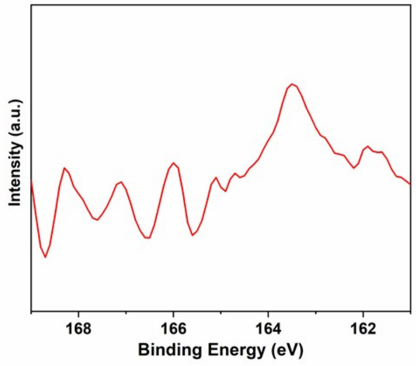

Figure S5. XPS profile of the sulfided FeO$_x$@Pd$_n$ sample showing the presence of sulfides.

References:

[S1] H.S. Fogler, Elements of chemical reaction engineering, 4th Ed., Prentice Hall, 2005.R.E.

[S2] J. Perez-Ramirez, R.J. Berger, G. Mul, F. Kapteijn, J.A. Moulijn, Catal. Today 60 (2000) 93.

[S3] J.F. Le Page, Applied heterogeneous catalysis, TechniP, 1987.

[S4] Q. Yu, L. Zhang, R. Guo, J. Sun, W. Fu, T. Tang, T. Tang, Fuel Process. Technol. 159 (2017) 76-87.

[S5] A. Niquille-Röthlisberger, R. Prins, J. Catal. 242 (2006) 207–216.

[S6] C. M. Van Den Bleek, K. Van Der Wiele and P. J. Van Den Berg, Chem. Eng. Sci. 24 (1969) 681–694